The genome of the seagrass Zostera marina reveals angiosperm adaptation to the sea

Jeanine L. Olsen, Pierre Rouzé, Bram Verhelst, Yao-Cheng Y.-C. Lin, Till Bayer, Jonas Collen, Emanuela Dattolo, Emanuele de Paoli, Simon Dittami, Florian Maumus, et al.

LETTER

OPEN

doi:10.1038/nature16548

The genome of the seagrass *Zostera marina* reveals angiosperm adaptation to the sea

Jeanine L. Olsen[1]*, Pierre Rouzé[2], Bram Verhelst[2], Yao-Cheng Lin[2], Till Bayer[3], Jonas Collen[4], Emanuela Dattolo[5], Emanuele De Paoli[6], Simon Dittami[4], Florian Maumus[7], Gurvan Michel[4], Anna Kersting[8,9], Chiara Lauritano[5], Rolf Lohaus[2], Mats Töpel[10], Thierry Tonon[4], Kevin Vanneste[2], Mojgan Amirebrahimi[11], Janina Brakel[3], Christoffer Boström[12], Mansi Chovatia[11], Jane Grimwood[11,13], Jerry W. Jenkins[11,13], Alexander Jueterbock[14], Amy Mraz[15], Wytze T. Stam[1], Hope Tice[11], Erich Bornberg-Bauer[8], Pamela J. Green[16], Gareth A. Pearson[17], Gabriele Procaccini[5]*, Carlos M. Duarte[18], Jeremy Schmutz[11,13], Thorsten B. H. Reusch[3,19]* & Yves Van de Peer[2,20,21]*

Seagrasses colonized the sea[1] on at least three independent occasions to form the basis of one of the most productive and widespread coastal ecosystems on the planet[2]. Here we report the genome of *Zostera marina* (L.), the first, to our knowledge, marine angiosperm to be fully sequenced. This reveals unique insights into the genomic losses and gains involved in achieving the structural and physiological adaptations required for its marine lifestyle, arguably the most severe habitat shift ever accomplished by flowering plants. Key angiosperm innovations that were lost include the entire repertoire of stomatal genes[3], genes involved in the synthesis of terpenoids and ethylene signalling, and genes for ultraviolet protection and phytochromes for far-red sensing. Seagrasses have also regained functions enabling them to adjust to full salinity. Their cell walls contain all of the polysaccharides typical of land plants, but also contain polyanionic, low-methylated pectins and sulfated galactans, a feature shared with the cell walls of all macroalgae[4] and that is important for ion homoeostasis, nutrient uptake and O_2/CO_2 exchange through leaf epidermal cells. The *Z. marina* genome resource will markedly advance a wide range of functional ecological studies from adaptation of marine ecosystems under climate warming[5,6], to unravelling the mechanisms of osmoregulation under high salinities that may further inform our understanding of the evolution of salt tolerance in crop plants[7].

Seagrasses are a polyphyletic assemblage of basal monocots belonging to four families in the Alismatales[1,2] (Supplementary Note 1.1 and Supplementary Fig. 1.1). As a functional group, they provide the foundation of highly productive ecosystems present along the coasts of all continents except Antarctica, where they rival tropical rain forests and coral reefs in ecosystem services[8,9]. In colonizing sedimentary shorelines of the world's ocean, seagrasses found a vast new habitat free of terrestrial competitors and insect pests but had to adapt to cope with new structural and physiological challenges related to full marine conditions.

Zostera marina (Zosteraceae), or eelgrass (Fig. 1), is the most widespread species throughout the temperate northern hemisphere of the Pacific and Atlantic[10]. A clone of *Z. marina* was sequenced from the Archipelago Sea, southwest Finland, using a combination of fosmid-ends and whole-genome shotgun (WGS) approaches (Methods, Supplementary Note 2). The 202.3 Mb *Z. marina* genome encodes 20,450 protein-coding genes, 86.6% of which (17,511 genes, Supplementary Note 3.1) are supported by transcriptome data from leaves, roots and flowers (Extended Data Fig. 1, Supplementary Notes 3.2–3.3 and Supplementary Data 1–3). Genes are located in numerous gene-dense islands separated by stretches of repeat elements accounting for 63% of the non-gapped assembly (Extended Data Fig. 2, Supplementary Note 3.1) as compared to only 13% in the only other sequenced alismatid, the freshwater duckweek, *Spirodela polyrhiza* (Alismatales, Araceae)[11]. Gypsy-type (32%) and Copia-type (20%) transposable elements contribute to most of the repetitive DNA. Sequence divergence analysis suggests that the genome retains copies from two distinct periods of invasion by Copia elements, but only one period for Gypsy elements (Extended Data Fig. 3a–c). Genes gained by *Z. marina* ('accessory') are located closer to transposable elements than to conserved ('single copy') genes (Fisher's exact test, $P < 0.0001$) indicating that transposable elements may have played a role in genic adaptation.

We identified 36 conserved microRNAs with high confidence and their predicted targets (Supplementary Note 3.4, Supplementary Data 4 and 5). A novel variant of miR528 (not present in *Spirodela*) was found to be the only member of this miRNA family, and demonstrates that this conserved miRNA is the only one ancestral to the entire monocot lineage. Most likely, *Z. marina* did not take part in the subsequent birth of miRNAs that are common to several other monocots[12]; nor did it experience or retain traces of prominent miRNA duplications.

Analysis of synonymous substitutions per synonymous site (K_S) age distributions indicates that *Z. marina* carries the remnants of an independent, ancient whole-genome duplication (WGD) event (Fig. 2a, Supplementary Note 4.1)[13]. Duplicated segments account for ~9% of the *Z. marina* genome, probably an underestimate due to the fragmented nature of the assembly. *Zostera* and *Spirodela* diverged somewhere between 135 and 107 million years ago (Mya)[14] and

[1]Groningen Institute of Evolutionary Life Sciences (GELIFES), University of Groningen, PO Box 11103, 9700 CC Groningen, The Netherlands. [2]Department of Plant Systems Biology, VIB and Department of Plant Biotechnology and Bioinformatics, Ghent University, Technologiepark 927, B-9052 Ghent, Belgium. [3]GEOMAR Helmholtz Centre for Ocean Research-Kiel, Evolutionary Ecology, Düsternbrooker Weg 20, D-24105 Kiel, Germany. [4]Sorbonne Université, UPMC Univ Paris 06, CNRS, UMR 8227, Integrative Biology of Marine Models, Station Biologique de Roscoff, CS 90074, F-29688, Roscoff cedex, France. [5]Stazione Zoologica Anton Dohrn, Villa Comunale, 80121 Naples, Italy. [6]Dipartimento di Scienze Agrarie e Ambientali, University of Udine, Via delle Scienze 206, 33100 Udine, Italy. [7]INRA, UR1164 URGI—Research Unit in Genomics-Info, INRA de Versailles-Grignon, Route de Saint-Cyr, Versailles 78026, France. [8]Institute for Evolution and Biodiversity, Westfälische Wilhelms-University of Münster, Hüfferstrasse 1, D-48149 Münster, Germany. [9]Institute for Computer Science, Heinrich Heine University, D-40255 Duesseldorf, Germany. [10]Department of Biological and Environmental Sciences, Bioinformatics Infrastructure for Life Sciences (BILS), University of Gothenburg, Medicinaregatan 18A, 40530 Gothenburg, Sweden. [11]Department of Energy Joint Genome Institute, 2800 Mitchell Dr., #100, Walnut Creek, California 94598, USA. [12]Environmental and Marine Biology, Faculty of Science and Engineering, Åbo Akademi University, Artillerigatan 6, FI-20520 Turku/Åbo, Finland. [13]HudsonAlpha Institute for Biotechnology, 601 Genome Way NW, Huntsville, Alabama 35806, USA. [14]Marine Ecology Group, Nord University, Postbox 1490, 8049 Bodø, Norway. [15]Amplicon Express, 2345 NE Hopkins Ct., Pullman, Washington 99163, USA. [16]School of Marine Science and Policy, Department of Plant and Soil Sciences, Delaware Biotechnology Institute, University of Delaware, 15-Innovation Way, Newark, Delaware 19711, USA. [17]Marine Ecology and Evolution, Centre for Marine Sciences (CCMAR), University of Algarve, 8005-139 Faro, Portugal. [18]King Abdullah University of Science and Technology (KAUST), Red Sea Research Center (RSRC), Thuwal 23955-6900, Saudi Arabia. [19]University of Kiel, Faculty of Mathematics and Natural Sciences, Christian-Albrechts-Platz 4, 24118 Kiel, Germany. [20]Genomics Research Institute, University of Pretoria, Hatfield Campus, Pretoria 0028, South Africa. [21]Bioinformatics Institute Ghent, Ghent University, Ghent B-9000, Belgium.
*These authors contributed equally to this work.

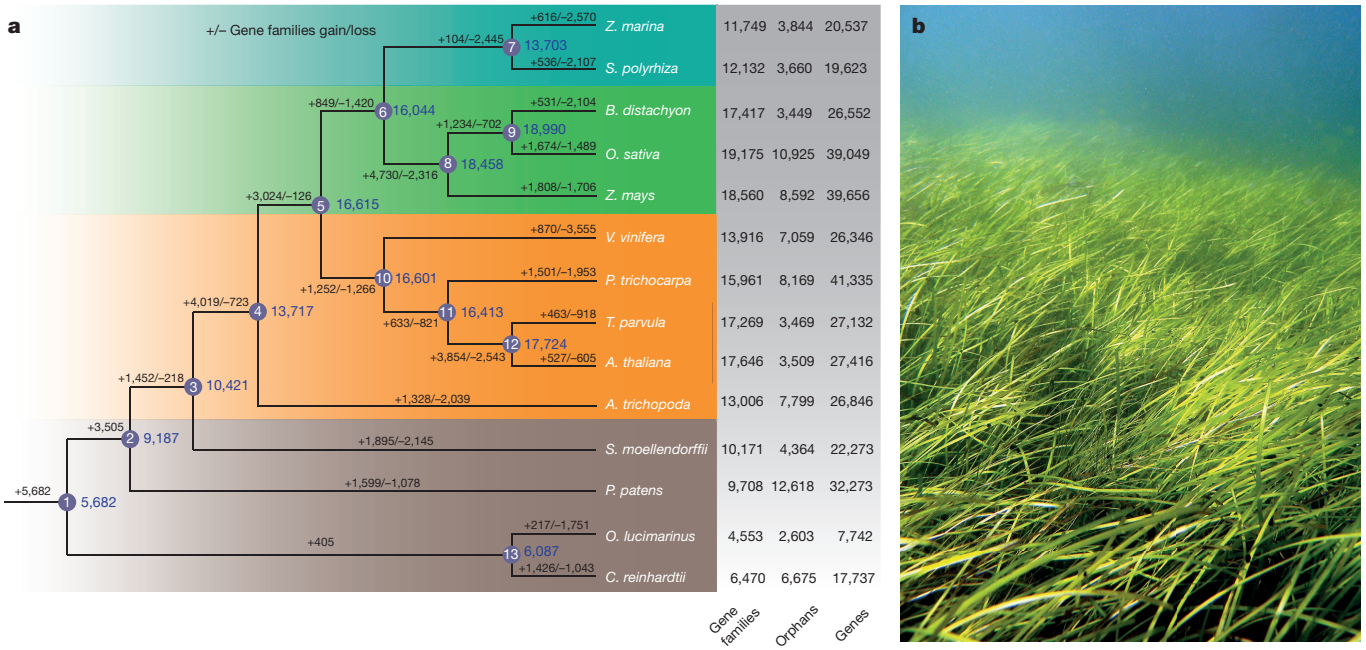

Figure 1 | *Zostera marina* and phylogenetic tree showing gene family expansion/contraction analysis compared with 13 representatives of the Viridiplantae. a, Gains and losses are indicated along branches and nodes. The number of gene families, orphans (single-copy gene families) and number of predicted genes is indicated next to each species. Background colours (top to bottom) are Alismatales, other monocots, dicots, mosses/algae **b**, Typical *Zostera marina* meadow, Archipelago Sea, southwest Finland (photo by C.B.).

phylogenomic dating[13] of the *Z. marina* WGD suggests that it occurred 72–64 Mya (Fig. 2b), thus independently from the two WGDs reported for *S. polyrhiza*[11]. This timeframe coincides with the initial diversification of a freshwater clade that includes three of the four families of seagrasses (Supplementary Table 1.1) and with the Cretaceous–Palaeogene (K–Pg) extinction event (Fig. 2c), which provided new ecological opportunities and may have triggered seagrass adaptive radiations.

We mapped signatures of loss and gain of gene families (Supplementary Note 4.2) onto a phylogenetic tree (Fig. 1a). We also mapped losses and gains of Pfam domains (Supplementary Fig. 4.4, Supplementary Data 6). While many genes are shared between *Zostera* and *Spriodela*, clearly some losses and gains are unique to *Zostera* in relation to its marine environment, the alismatid lineage having set the stage for the subsequent freshwater–marine transition. Those unique to *Z. marina* include the absence of all the genes involved in stomatal differentiation (Fig. 3a, Extended Data Table 1 and Supplementary Note 5.1) and the disappearance of genes comprising entire pathways encoding volatiles synthesis and sensing (Supplementary Note 6.1), such as those for ethylene[15] (Fig. 3b, Extended Data Table 2). Terpenoid genes are also drastically reduced to two (Fig. 3c), as compared with four in *Spirodela*, 50 in *Oryza* and > 100 in *Eucalyptus*, thus

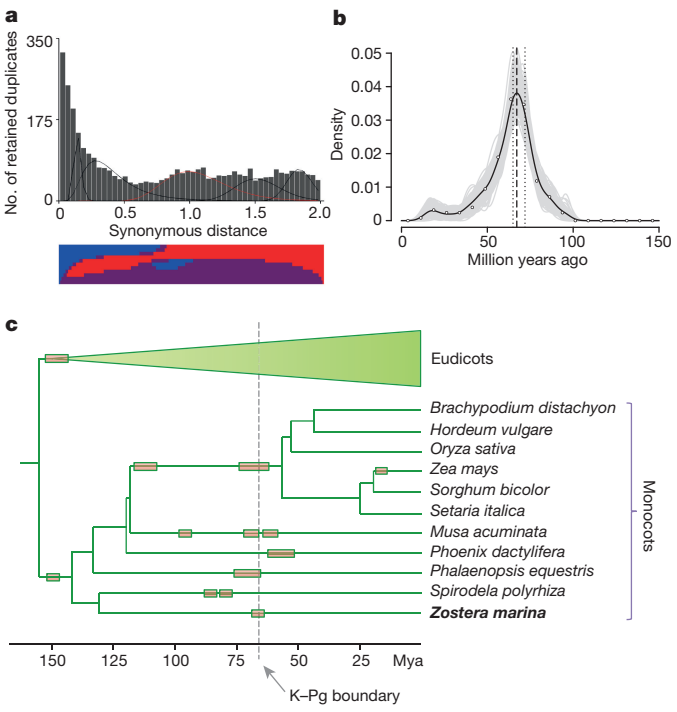

Figure 2 | Ancient whole-genome duplication (WGD). a, K_S-based age distribution of the whole *Z. marina* paranome. The *x* axis shows the synonymous distance until a K_S cut-off of 2, in bins of 0.04, containing the K_S values that were used for mixture modelling (excluding those with a $K_S \leq 0.1$). The component of the Gaussian mixture model plotted in red (as identified by EMMIX) corresponds to a WGD feature based on the SiZer analysis (other components are shown in black). The transition from the blue to the red at a K_S of ~0.8 in the SiZer panel (below) indicates a change in the distribution and therefore provides evidence for an ancient WGD (Supplementary Table 4.1, Supplementary Fig. 4.1). **b**, Absolute age distribution obtained by phylogenomic dating of *Z. marina* paralogues. The solid black line represents the kernel density estimate (KDE) of the dated paralogues and the vertical dashed black line represents its peak, used as the consensus WGD age estimate, at 67 Mya. Grey lines represent the density estimates from 2,500 bootstrap replicates and the vertical black dotted lines represent the corresponding 90% confidence interval for the WGD age estimate, 64–72 Mya. The original raw distribution of dated paralogues is indicated by the circles. The *y* axis represents the percentage of gene pairs. **c**, Pruned phylogenetic tree with indication of WGD events (boxes)[29]. The Cretaceous–Palaeogene (K–Pg) boundary is indicated by an arrow.

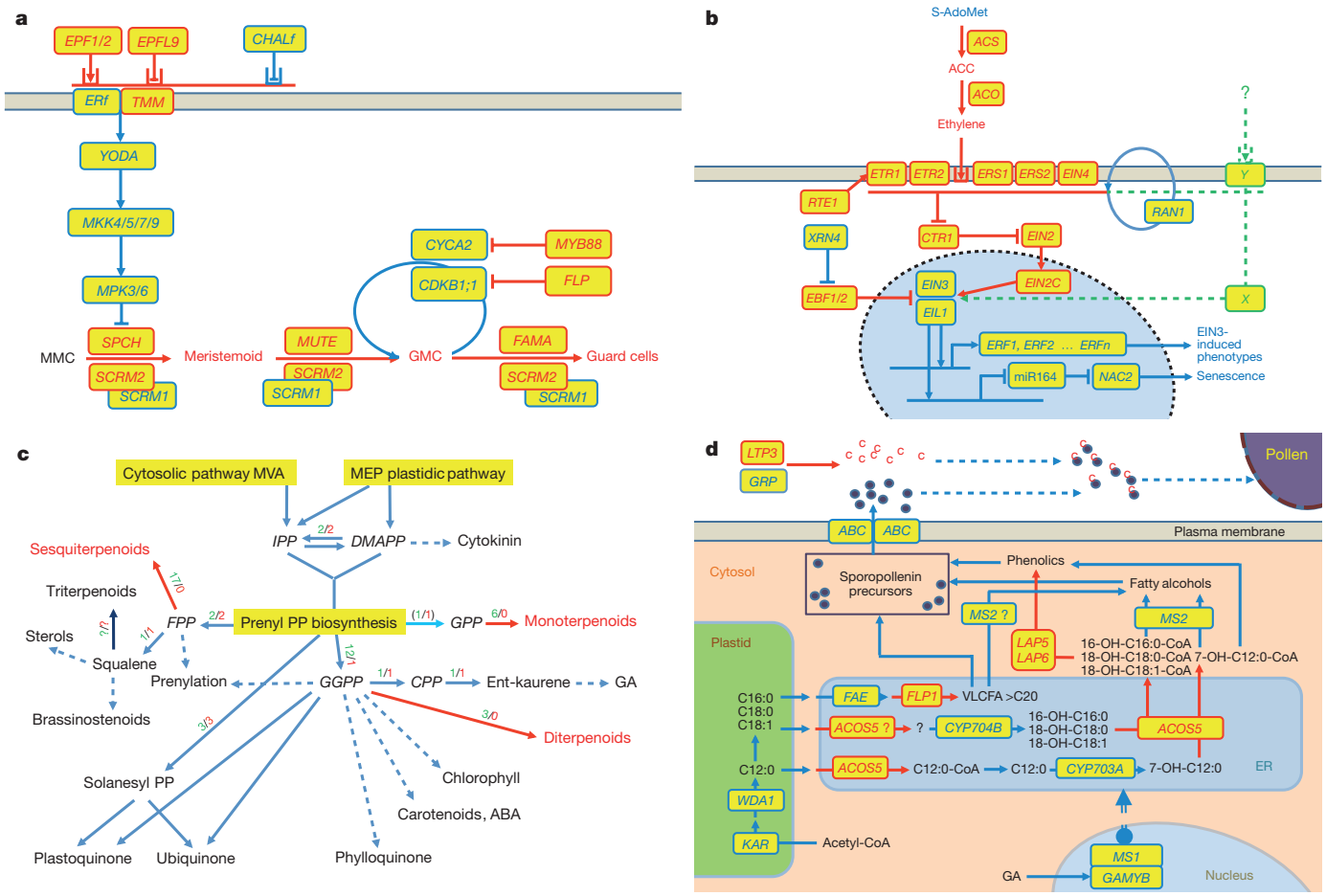

Figure 3 | Reconstruction of metabolic (or gene) pathways involved in the production of stomata, ethylene, terpene and pollen in *Z. marina*. **a**, Stomata differentiation from meristemoid mother cells (MMC) to guard mother cell (GMC) to guard cells. **b**, Ethylene synthesis and signalling up to *EIN2* have disappeared; *EIN3* and its downstream targets remain. **c**, Terpenoid biosynthesis in which the pathways producing volatiles are absent but those essential for primary metabolism remain. MVA, mevalonate; MEP, plastidic methylerythritol phosphate; IPP, isopentenyl pyrophosphate; DMAPP, dimethylallyl pyrophosphate; FPP, farnesyl pyrophosphate; GPP, geranyl diphosphate; GGPP, geranylgeranyl pyrophosphate; CPP, copalyl pyrophosphate; GA, gibberellic acid; PP, diphosphate; ABA, abscisic acid. **d**, Sporopollenin biosynthesis genes; regulatory genes in the nucleus control downstream processes (arrows) in response to signalling coming from external stimuli through receptors on the plasma membrane. All panels: genes in red are absent; blue are present; the grey line represents the plasma membrane. See Extended Data Tables 1–3.

precluding synthesis of secondary volatile terpenes (Supplementary Fig. 6.2). Only aromatic acid decarboxylases (AAAD) genes were expanded (Supplementary Fig. 6.3) and these form a clade distinct from *Spirodela*. The loss of volatiles is also consistent with the loss of stomata, through which they are emitted for airborne communication and plant defence. The repertoire of defence-related genes such as the six groups of NBS_LRR resistance genes (Supplementary Note 6.2) is also reduced to 44 (89 in *Spirodela* and 100–300 in other plants), which may be linked to a lower probability of infection of *Z. marina* due to the absence of stomata, which are a main entry point for pests and pathogens in terrestrial plants.

Land and aquatic floating plants (Embryophyta) are often exposed to intense ultraviolet (UV) radiation and have developed light sensing protein receptors with protective and signalling functions. In contrast, *Z. marina* inhabits a light-attenuated, submarine environment where it must cope with shifted spectral composition, characterized by low penetration of UV-B, red and far-red wavelengths[16]. Accordingly, *Z. marina* has lost ultraviolet-resistance (UVR8) genes associated with sensing and responding to UV damage (*Spirodela* has not), as well as phytochromes associated with red/far-red receptors (Supplementary Note 7). Whereas photosystems (PSI and PSII) are similar to those of other plants including *Spirodela*, members of the light-harvesting complex B (LHCB) family are expanded in number, possibly in combination with non-photochemical quenching (NPQ), thereby enhancing performance at low light (Extended Data Fig. 4).

Seagrasses typically experience full marine seawater (35 g kg^{-1})[17], whereas land plants obtain water with low osmolality (0–2 g kg^{-1}) via the rhizosphere and aquatic plants experience fresh (0–5 g kg^{-1}) to brackish (0.5–20 g kg^{-1}) conditions. Although *Z. marina* displays a typical repertoire of Na^+ and K^+ antiporters (Supplementary Note 8, Supplementary Table 8.1), one of six H^+-ATPase (AHA) genes (Supplementary Table 8.2, Supplementary Data 7) is strongly expressed in vegetative tissue and encodes a salt-tolerant H^+-ATPase. Furthermore, *Z. marina* possesses three AHA genes (along with *Spirodela*) in a cluster unique to alismatids (Supplementary Fig. 8.1).

Uniquely, *Z. marina* has re-evolved new combinations of structural traits related to the cell wall. Synthesis of cutin-cuticular waxes to the outside of the leaf epidermis and suberin–lignin near the plasma membrane (Supplementary Note 9, Supplementary Table 9.1) surround a cell wall matrix of (hemi)celluloses, low-methylated pectin (zosterin) and macroalgal-like sulfated polysaccharides[18] (Supplementary Note 10). The reduction in carbohydrate-related genes that modify the fine structure of cell wall hemicelluloses and pectins in *Z. marina* is not due to loss of pathways, but rather to the large variation within these CAZyme gene families in plants. Available genomes (including *Spirodela*) lack carbohydrate sulfotransferases and sulfatases, suggesting that land

plants have lost these genes as a key adaptation to terrestrial as well as freshwater conditions[19,20]. In contrast, *Z. marina* has regained the ability to produce sulfated polysaccharides with an expansion of aryl sulfotransferases (12 genes) homologous to aryl sulfotransferases from land plants (Supplementary Note 10). Sulfation facilitates water and ion retention in the cell wall to cope with desiccation and osmotic stress at low tide and, likewise, low methylation of zosterin correlates with the expanded pectin carbohydrate esterase 8 (CE8) family, increasing the polyanionic character of the cell wall matrix. We speculate that several aryl sulfotransferases have evolved because carbohydrate sulfatases have been shown to be active on artificial aryl compounds such as methylumbelliferyl-sulfate[21]. Osmotic equilibrium is further achieved in *Z. marina* by organic osmolytes (mainly sucrose, trehalose and proline) in combination with a small cytoplasm:vacuole volume ratio (10%)[22]. Given that up to 90% of fixed carbon is stored as sucrose in the rhizomes, sucrose synthase (SuSy) and transport (SUT) genes are expanded while those for starch metabolism are greatly reduced, as expected in 'marine sugarcane' (Supplementary Note 7.2, Supplementary Data 8).

The repertoire of redox and other stress-resistance genes (Supplementary Note 8) is typical for angiosperms with the exception of catalase (CAT), which is reduced to a single copy in *Z. marina* (two in *Spirodela*). Late embryogenesis abundant (LEA) and dehydrins are clearly under-represented in both *Zostera* and *Spriodela* relative to other genomes. In contrast, *Zostera* possesses an unusual complement of metallothioneins. Aside from their role as chelators, metallothioneins may be involved in stress resistance; one of these, MT2L, is among the most highly constitutively expressed genes in *Z. marina* (Extended Data Fig. 5, Supplementary Note 8.2).

Sexual reproduction of *Z. marina* takes place underwater, involving completely submerged male and female flowers, and a unique exine-less, filiform pollen that winds around the bifurcate stigmas in a purely abiotic pollination process[23]. Note that freshwater alismatids (and also *Spirodela*)[24] possess pollen with an exine layer. Exine-less pollen[25] is characteristic of all seagrasses except *Enhalus acoroides* (which is surface pollinated). Ten genes specifically involved in biosynthesis and modification of the pollen exine coat are missing; all other genes involved in the development of viable pollen remain intact (Fig. 3d, Extended Data Table 3, Supplementary Note 11.1). Finally, MADS-box gene transcription factors are also highly reduced to 50 in *Z. marina*, which is most likely related to its highly reduced flowers (also a feature of *Spirodela)* that lack the first two whorls of specialized floral leaves, calyx and corolla (Supplementary Note 11.2, Supplementary Table 11.2).

An increasing proportion of the world population inhabits the coastal zone. This impinges multiple pressures on ecosystems including seagrass beds[26,27], which in turn compromises the ecosystem services they may provide, including provisioning of harvestable fish and invertebrates, nutrient retention, carbon sequestration and erosion control. In the context of seagrass conservation, elucidating the genomic basis of *Z. marina*'s complex adaptations to ocean waters (Extended Data Fig. 6) will also inform the development of molecular indicators of their physiological status[28], as these unique ecosystems rank, unfortunately, among the most threatened on Earth[26,27].

Online Content Methods, along with any additional Extended Data display items and Source Data, are available in the online version of the paper; references unique to these sections appear only in the online paper.

Received 22 May; accepted 18 December 2015.
Published online 27 January 2016.

1. Les, D. H., Cleland, M. A. & Waycott, M. Phylogenetic studies in Alismatidae, II: evolution of marine angiosperms (seagrasses) and hydrophily. *Syst. Bot.* **22,** 443–463 (1997).
2. Larkum, W. D., Orth, R. J. & Duarte, C. M. *Seagrasses: Biology, Ecology and Conservation* (Springer, Dordrecht, Netherlands, 2006).
3. Berry, J. A., Beerling, D. J. & Franks, P. J. Stomata: key players in the earth system, past and present. *Curr. Opin. Plant Biol.* **13,** 232–239 (2010).
4. Aquino, R. S., Landeira-Fernandez, A. M., Valente, A. P., Andrade, L. R. & Mourao, P. A. S. Occurrence of sulfated galactans in marine angiosperms: evolutionary implications. *Glycobiology* **15,** 11–20 (2005).
5. Franssen, S. U. *et al.* Transcriptomic resilience to global warming in the seagrass *Zostera marina*, a marine foundation species. *Proc. Natl Acad. Sci. USA* **108,** 19276–19281 (2011).
6. Mazzuca, S. *et al.* Establishing research strategies, methodologies and technologies to link genomics and proteomics to seagrass productivity, community metabolism, and ecosystem carbon fluxes. *Front. Plant Sci.* **4,** 1–19 (2013).
7. Duarte, C. M. *et al.* Will the oceans help feed humanity? *Bioscience* **59,** 967–976 (2009).
8. Costanza, R. *et al.* The value of the world's ecosystem services and natural capital. *Nature* **387,** 253–260 (1997).
9. Fourqurean, J. W. *et al.* Seagrass ecosystems as a globally significant carbon stock. *Nature Geosci.* **5,** 505–509 (2012).
10. Green, E. P. & Short, F. T. *World Atlas of Seagrasses* (University of California Press, Berkeley, CA, USA, 2003).
11. Wang, W. *et al.* The *Spirodela polyrhiza* genome reveals insights into its neotenous reduction fast growth and aquatic lifestyle. *Nature Commun.* **5,** 1–13 (2014).
12. Chavez Montes, R. A. *et al.* Sample sequencing of vascular plants demonstrates widespread conservation and divergence of microRNAs. *Nature Commun.* **5,** 1–15 (2014).
13. Vanneste, K., Maere, S. & Van de Peer, Y. Tangled up in two: a burst of genome duplications at the end of the Cretaceous and the consequences for plant evolution. *Philos. Trans. R. Soc. B Biol. Sci.* **369,** 20130353 (2014).
14. Nauheimer, L., Metzler, D. & Renner, S. S. Global history of the ancient monocot family Araceae inferred with models accounting for past continental positions and previous ranges based on fossils. *New Phytol.* **195,** 938–950 (2012).
15. Golicz, A. A. *et al.* Genome-wide survejy of the seagrass *Zostera muelleri* suggests modification of the ethylene signalling network. *J. Exp. Bot.* (2015).
16. Kirk, J. T. O. in *Light and Photosynthesis in Aquatic Ecosystems* (Cambridge Univ. Press, 2011).
17. Touchette, B. W. Seagrass-salinity interactions: physiological mechanisms used by submersed marine angiosperms for a life at sea. *J. Exp. Mar. Biol. Ecol.* **350,** 194–215 (2007).
18. Popper, Z. A. *et al.* Evolution and diversity of plant cell walls: from algae to flowering plants. *Annu. Rev. Plant Biol.* **62,** 567–590 (2011).
19. Michel, G., Tonon, T., Scornet, D., Cock, J. M. & Kloareg, B. The cell wall polysaccharide metabolism of the brown alga *Ectocarpus siliculosus:* insights into the evolution of extracellular matrix polysaccharides in eukaryotes. *New Phytol.* **188,** 82–97 (2010).
20. Collen, J. *et al.* Genome structure and metabolic features in the red seaweed *Chondrus crispus* shed light on evolution of the Archaeplastida. *Proc. Natl Acad. Sci. USA* **110,** 5247–5252 (2013).
21. Hanson, S. R., Best, M. D. & Wong, C. H. Sulfatases: structure, mechanism, biological activity, inhibition, and synthetic utility. *Angew. Chem. Int. Ed.* **43,** 5736–5763 (2004).
22. Larkum, A. W. D., Drew, E. A. & Ralph, P. J. in *Seagrasses: Biology, Ecology and Conservation* (eds Larkum, A. W. D., Orth, R. J. & Duarte, C. M.) 323–345 (Springer, Dordrecht, Netherlands, 2006).
23. De Cock, A. W. Flowering, pollinations and fruiting in *Zostera marina* L. *Aquat. Bot.* **9,** 201–220 (1980).
24. Furness, C. A. in *Early Events in Monocot Evolution* (eds Wilkin, P. & Mayo, S. J.) 1–22 (Cambridge Univ. Press, 2013).
25. Kuo, J. & den Hartog, C. in *Seagrasses: Biology, Ecology and Conservation* (eds Larkum, A. W. D., Orth, R. J. & Duarte, C. M.) 51–87 (Springer, 2006).
26. Orth, R. J. *et al.* A global crisis for seagrass ecosystems. *Bioscience* **56,** 987–996 (2006).
27. Waycott, M. *et al.* Accelerating loss of seagrasses across the globe threatens coastal ecosystems. *Proc. Natl Acad. Sci. USA* **106,** 12377–12381 (2009).
28. Macreadie, P. I., Schliepl, M. T., Rasheed, M. A., Chartrand, K. M. & Ralph, P. J. Molecular indicators of chronic seagrass stress: a new era in the management of seagrass ecosystems? *Ecol. Indic.* **38,** 279–281 (2014).
29. Vanneste, K., Baele, G., Maere, S. & Van de Peer, Y. Analysis of 41 plant genomes supports a wave of successful genome duplications in association with the Cretaceous–Paleogene boundary. *Genome Res.* **24,** 1334–1347 (2014).

Supplementary Information is available in the online version of the paper.

Acknowledgements Genome sequencing, assembly and automated annotation were conducted by the US Department of Energy (DOE) Joint Genome Institute, Walnut Creek California, USA and supported by the Office of Science of the US DOE, Community Sequencing Program award (2009) contract No. DE-AC02-05CH11231 to J.L.O. Further bioinformatics and annotation was supported in part by the Ghent University Multidisciplinary Research Partnership 'Bioinformatics: From Nucleotides to Networks' to Y.V.d.P. Y.V.d.P also acknowledges support from the European Union Seventh Framework Programme (FP7/2007-2013) under European Research Council Advanced Grant Agreement 322739–DOUBLE-UP. RNA-seq (Finnish clone genotype) was funded by the Marine Benthic Ecology and Evolution (MarBEE) group, within the former Centre for Ecological and Evolutionary Studies (now Groningen Institute for Evolutionary Life Sciences), University of Groningen to J.L.O.

RNA-seq (flower tissues) was funded by the Excellence Cluster, Future Ocean, Kiel to T.B.H.R. Participation of G.P. and E.D. was supported by the MIUR Italian Flagship project RITMARE (NRP 2011-2013). G.A.P. was supported by FCT-EXCL/AAG-GLO/0661/2012. We thank I. D. Gromicho, KAUST, for his artistry in the production of Extended Data Fig. 6. This work also benefited from discussions within the ESSEM COST action ES0906, "Seagrass productivity from genes to ecosystem management" (2009-2014), J.L.O., G.P. and T.B.H.R; and the Linnaeus Centre for Marine Evolutionary Biology (CEMEB)-Tjärnö, Gothenburg University, J.L.O. and M.T. J.L.O. especially thanks K. Johannesson (CeMEB-Tjärnö), C. Boyen (SBR-Roscoff), R. Reinhardt (MPI-Cologne) and E. Serrão (CCMAR-Faro) for their ongoing encouragement, and the more than 70 colleagues who submitted letters of support for the original proposal to the JGI-Community Sequencing Program.

Author Contributions J.L.O., T.B.H.R., G.P. and Y.V.d.P. are the lead investigators and contributed equally to the work. J.S., J.W.J., J.G., Y.V.d.P., B.V. and Y.-C.L. coordinated the bioinformatics activities surrounding assembly, quality control, set-up and maintenance of *Z. marina* on the ORCAE site and deposition of the *Z. marina* genome resource. T.B.H.R and T.B. generated and analysed RNA-seq libraries from flowers, rhizome, roots. J.L.O., Y.-C.L. and A.J. generated and analysed RNA-seq libraries from the genome genotype and temperature stress experiments. C.B., W.T.S. and J.L.O. contributed to biological sample collection, preparation and quality control prior to DNA extraction. A.M. performed the HMW DNA extraction and quality control from the genome genotype/ clone. M.A., J.G., H.T. and M.C. contributed to WGS libraries and sequencing, (fosmid)-cloning and quality control. J.G. coordinated the sequencing of FES, quality control projects. Analysis of architectural features of the genome and annotation of specific gene families, including the written contributions to the main paper and Supplementary Information sections, were performed by the following co-authors: J.W.J., the chromosome assembly analysis; B.V. and Y.-C.L., gene family clustering and comparative phylogenomics; A.R.K. and E.B.B., Pfam domains; E.D.P. and P.J.G., miRNA; R.L., K.V. and Y.V.d.P., whole-genome duplication; F.M., Y.-C.L. and Y.V.d.P., transposable elements; B.V., co-linearity and synteny comparisons; M.T., organellar genomes; P.R., stomata gene family; G.M., cell wall polysaccharides and sulfotransferases; T.T., fatty acid metabolism and its relationship to cell walls and ion homeostasis; P.R., volatiles (ethylene, terpenes); P.R., J.B. and T.B.H.R., metallothioniens; P.R., G.A.P. and C.L., osmoregulation/ion homeostasis/stress-related genes; S.D. and E.D., photosynthetic/ light-sensing genes; G.M., CAZymes; T.B., T.B.H.R. and P.R., plant defence-related; T.B. assembly and analysis of MADS box genes (flowering); P.R.; Y.V.d.P. and Y.-C.L., pollen-related and self-incompatibility genes; F.M., SLR-1gene and core eukaryotic genes analysis (CEGMA). J.L.O., Y.V.d.P., T.B.H.R., C.M.D., Y.-C.L. and P.R. wrote and edited the main manuscript (including the Methods and Extended Data), and organized and further edited the individual contributions (as listed above) for the Supplementary Information sections. J.L.O. and Y.V.d.P. provided the overall evolutionary context and T.B.H.R., G.P. and C.M.D. provided the ecological and societal context. All authors read and commented on the manuscript.

Author Information Raw reads, the assembled genome sequence and annotation are accessible from NCBI under BioProject number PRJNA41721 with GenBank accession number LFYR00000000. The accession number for the *Zostera marina* Finnish Clone is BioSample SAMN00991190. Fosmid end sequence: GSS KG963492–KG999999; KO000001–KO144970, whole-genome shotgun data: SRA020075 and RNA-seq: GEO GSE67579. Further information on the *Zostera marina* project is available via the Online Resource for Community Annotation Eukaryotes (ORCA) at http://bioinformatics.psb.ugent.be/orcae/. Reprints and permissions information is available at www.nature.com/reprints. The authors declare no competing financial interests. Readers are welcome to comment on the online version of the paper. Correspondence and requests for materials should be addressed to J.L.O. (j.l.olsen@rug.nl) or Y.V.D.P (yves.vandepeer@psb.vib-ugent.be).

METHODS

No statistical methods were used to predetermine sample size. The experiments were not randomized and the investigators were not blinded to allocation during experiments and outcome assessment.

Plant material and DNA preparation. A single genotype/clone of *Zostera marina* (referred to as the 'Finnish clone') was harvested on 26 August 2010 at 2 m depth at Fårö Island (latitude 59° 55.234′ N longitude 21° 47.766′ E) located in the northern Baltic Sea, Finland. Plant material was transported to the lab in seawater, cleaned and further processed. Care was taken to use leaf-meristem tissue harvested from the inner layer of basal shoots to minimize bacterial/diatom contamination. Tissues were immediately frozen in LN_2 and stored at −80 °C for later DNA and RNA extraction. Monoclonality was verified by genotyping 40 ramets of the mega-clone with six highly polymorphic, microsatellite loci[30]. There was no evidence for polyploidy[25,31,32] (*Z. marina* is 2n = 12) or somatic mutations[33] as assessed by multiple peaks in the microsatellite chromatograms. Tissue was subsequently sent on dry ice to Amplicon Express for HMW DNA extraction using a CTAB isolation method modified by R. Meilan (unpublished) but available from him (rmeilan@purdue.edu), based on the original method[34]. Following QC according to JGI guidelines, the DNA was shipped to JGI for library and sequencing preparation.

Genome sequencing and assembly. One 35-Kb, fosmid library was generated for end sequencing. The fosmid ends were sequenced with standard Sanger sequencing protocols at the HudsonAlpha Institute for a total of 194,303 Sanger reads (0.29× coverage). Illumina libraries (two fragment libraries (6.62 Gb), one 2-Kb JGI mate-pair library (3.57 Gb), one 4-Kb JGI mate-pair library (3.41 Gb) and two 8-Kb JGI mate-pair libraries (11.94 Gb)) were sequenced with Illumina MiSeq/HiSeq genetic analysers at the Department of Energy's Joint Genome Institute (JGI), using standard protocols. A total of 25.55 Gb of Illumina and 0.14 Gb of Sanger sequence was obtained representing 47.7× genomic coverage. Prior to assembly, all reads were screened against mitochondria, chloroplast, and Illumina controls. Reads composed of >95% simple sequence repeats were removed. For the Illumina, paired-end libraries (2 × 250), reads <75 bp were discarded, for the 2 × 150 libraries, reads <50 bp were discarded after trimming for adaptor and quality ($q < 20$). An additional deduplication step was performed on the mate pairs that identified and retained only one copy of each PCR duplicate. A total of 212,101,273 reads (Supplementary Table 2.1) was assembled using our modified version of Arachne v. 20071016 (ref. 35). Subsequent directed Arachne modules were applied to collapse adjacent heterozygous contigs. The entire assembly was then run through another Arachne process starting at Stage 6 Rebuilder. This produced 15,747 scaffold sequences (30,723 contigs), with a scaffold L50 of 409.5 Kb, 613 scaffolds larger than 100 Kb, and a total genome size of 237.5 Mb (Supplementary Table 2.2).

Scaffolds were screened against bacterial proteins, organelle sequences, GenBank NR (nr_prot) and RefSeq protein databases, and removed if found to be a contaminant. Scaffolds consisting of prokaryotes, chloroplast, mitochondria and unanchored rDNA were removed. We also assembled the chloroplast and partial mitochondrial genomes (Supplementary Notes 2.2 and 2.3, Supplementary Fig. 2.1). Additionally, short (<1 Kb) scaffolds or scaffolds containing highly repetitive sequence (>95% 24-mers found more than four times in large scaffolds) or alternative haplotypes were also removed. Following repeat analysis and gene prediction, all scaffolds were subjected to a filtering process (based on NCBI nr_prot + NCBI taxonomy database) to eliminate remaining bacterial (and other) contaminants (Supplementary Table 2.3).

Assembly validation was performed using a set of 12 fully sequenced fosmid clones. In 4 of the 12 fosmid clones, full-length alignments were not found due to fragmentation in the region of the fosmid clone. In five of the remaining eight fosmid clones, the alignments were of high quality (<0.05% bp error). The overall base pair error rate (including marked gap bases) in the fosmid clones that aligned to full length was 0.28% (714 discrepant base pairs out of 253,332 bp). Supplementary Table 2.4 shows the individual fosmid clones and their contribution to the overall error rate. Note that two fosmid clones (16248, 16249) contributed nearly 81% of the discrepant bases. This probably occurred in polymorphic regions of the genome where the haplotype in the fosmid did not match the haplotype in the reference. There are several indels of various sizes in the clone and assembly, typical of a region of degraded transposons. Further quality analysis indicated that 90% of the set of eukaryotic core genes (CEGMA) were present and 98% were partially represented, suggesting near completeness of the euchromatin component.

Annotation of repetitive sequences. Two complementary approaches were used to identify repetitive DNA sequences in the *Z. marina* genome. With respect to masking repeats before gene prediction analysis, a *de novo* repeat identification was carried out with RepeatModeller (v. open-1.0.7; http://www.RepeatMasker.org)[36] to identify repeat boundaries and build consensus models from which potential over represented, non-transposable element, protein-coding genes were removed. RepeatMasker (v. open-4.0.0, WUBlast) was used in combination with this custom repeat library to mask the assembly and prepare it for gene prediction with EuGene.

Furthermore, in order to perform a qualitative and quantitative analysis of repeats with greater resolution[37] the genome assembly was processed for *de novo* repeat detection using the TEdenovo pipeline from the REPET package v. 2.2 (ref. 38); parameters were set to consider repeats with at least five copies. The consensus sequences generated by TEdenovo were then used as probes for whole genome annotation by the TEannot[39] pipeline from the REPET package v. 2.2. The consensus repeat sequences were classified using Pastec[40]. Comparing the genomic positions of transposable elements (TE) to those of exons from the set of predicted genes enabled us to identify that 909 gene predictions most likely represent TEs and these were filtered from the gene set. The REPET package v. 2.2 was also used to annotate repetitive elements in the *Spirodela polyrhiza* genome assembly with the same parameters as for *Z. marina*. See Supplementary Fig. 3.1.

Transcriptome library preparation, sequencing and assembly. Leaf, root and flower tissues were separately frozen in liquid nitrogen immediately following harvest from either ambient (field collected) or experimental (mesocosm) conditions (Supplementary Note 3.2). Overall, we obtained between nine and 20 million high-quality reads from each of the flower-leaf-root replicate libraries; and for the Finnish clone library, 148.5 million high quality reads were retrieved (Supplementary Table 3.3).

The *de novo* assembly protocol was adapted from ref. 41. We pooled replicates of each tissue together except for the two leaf tissue libraries, which were kept separate (Supplementary Table 3.4) and performed *de novo* transcriptome assembly for each tissue using Trinity[41](v. 2014-07-17) with digital normalization option ON to normalize input read coverage. Frame shift errors and insertion/deletion errors in the assembled transcripts were corrected by FrameDP[42]. Because a *de novo* assembly still generates many spurious transcripts, we used the transcript expression value to remove low quality contigs. We used the RSEM pipeline[43] to obtain the contig expression values and removed contigs with FPKM (fragments per kilobase of transcript per million fragments mapped) value <1 and IsoPct (percentage of expression for a given transcript compared with all expression from that Trinity component) < 1. In total, we obtained between 39,000 and 53,000 assembled contigs from each library, and 52,000 contigs from the Finnish clone library (Supplementary Table 3.4). Prior to mapping the genome sequence and the predicted genes, we used the CD-HIT[44] program (v. 4.6.1) to collapse redundant contigs, which resulted in 79,134 low redundant transcript contigs.

Differential gene expression analysis. High-quality RNA-seq reads were mapped to the genome assembly v.2.1 by TopHat[45]. Differential gene expression analysis was performed by the Cufflink pipeline[45] based on the *Z. marina* v.2.1 gene models by converting the number of aligned reads into FPKM values. Genes with significant expression difference ($\log_2 > 2$) were selected for further investigation by GOstats[46] to perform Gene Ontology (GO) term enrichment analysis with $P \leq 0.05$ (Supplementary Note 3.3, Supplementary Table 3.5)

MicroRNA analysis. Genomic precursors of known miRNAs were mapped on the *Z. marina* genome following the procedure described in ref. 47 for the maize genome. miRNA entries from the miRBase database (release 21, 2014) were aligned to the chromosomes of the *Z. marina* genome. Up to three mismatches were allowed in the alignment, using SeqMap[48]. In parallel, novel potential DCL1/AGO1-dependent miRNAs were enriched by selecting 5′-U 20–22 nt small RNAs from three different sequenced libraries from *Z. marina* described in ref. 12. A subset of these small RNAs with abundance ≥10 TPM (transcripts per million) was retained and aligned to the genome with no mismatches. From every locus, we extracted two ~200-nt regions surrounding each aligned miRNA or candidate (from −30 to +160 and from −160 to +30 nucleotides relative to the putative miRNA start or end coordinate, respectively). Minimum energy RNA secondary structures were predicted for each region using the RNAfold program of the Vienna RNA 1.8.5 package (http://www.tbi.univie.ac.at/~ivo/RNA/) using default settings.

In addition, small RNAs from the three sequenced libraries were mapped on these regions, allowing no mismatches, in order to pre-select putative miRNA loci that showed evidence of expression in the three plant tissues analysed. We evaluated RNA structure and small RNA alignment in all the regions based on: (1) dominance of plus-stranded small RNAs; (2) position of the most abundant small RNAs relative to the predicted miRNA coordinates; (3) prevalence of 20–22 nt small RNAs in the predicted miRNA locus; (4) position of the putative miRNA with the stem-loop structure; and (5) absence of oversize (≥3 nt) bulges in the miRNA/miRNA* alignment. After reduction of overlapping loci to a non-redundant set and removal of stem-loop structures with the wrong orientation compared to miRNAs registered in miRBase, we manually inspected the remaining loci to further evaluate them according to the miRNA annotation criteria proposed by ref. 49. Stringency was relaxed when small RNA expression data strongly indicated the presence of miRNA loci that did not meet the whole set of criteria. Novel miRNA precursors overlapping with TEs or other repetitive elements were filtered out.

Potential miRNA targets were identified *in silico* using the generic small RNA-transcriptome aligner GSTAr from the CleaveLand package (v. 4)[50]. Predicted targets were accepted with an Allen score <4 or a MFE (minimum free energy) ratio ≥7.5. (Supplementary Note 3.4).

Gene prediction. Training of the gene prediction programs started with the collection of high quality ESTs. EST information was used, for example, to train the splice predictor SpliceMachine[51]. Detection of conserved splice sites was further investigated by RNA-seq splice junctions (count > 10) to construct a WAM model in EuGene (v. 4.1)[52]. Coding-potential was modelled with an interpolated Markov Model (IMM) constructed from the BLASTX alignments of proteins from the PLAZA v. 2.5 database[53]. An additional protein 'monocot' Markov Model was built based on the protein sequences from *Brachypodium*, maize and sorghum. Starting from EST and protein alignments, a set of 215 gene models was manually constructed and curated using the genome browser GenomeView[54]. The 215 models were then used as a training set for EuGene in order to optimize the different splice site and coding-potential models, as well as the weights for the extrinsic EST and homology evidence. An overall fitness score of 80.1% was achieved, which is high enough to obtain reliable results without overfitting. GeneMark[55] and Augustus[56] were separately trained (using the same input data as EuGene) and their predictions were integrated with EuGene using a custom script to evaluate the best gene structure at each locus. All gene models were automatically screened to highlight possible erroneous structures (for example, in-frame stop codons, deviating splice junctions) and manually curated. Transfer-RNA gene models were predicted by tRNAscan-SE (v. 1.31)[57] and their structures were verified with Infernal (v. 1.1rc1, rfam11 covariant model database)[58]. For each gene, UTRs were assigned by identifying a set of ESTs and RNA-seq assemblies that uniquely overlapped with it. We subsequently selected the longest mapped transcript on either end of the predicted coding sequence and designated the section outside the coding sequence as the UTR. Finally, all genes were uploaded to the ORCAE platform (http://bioinformatics.psb.ugent.be/orcae)[59], enabling all members of the consortium to refine and curate the gene model and assign gene function. A list of protein domains, as well as the derived Gene Ontology (GO) terms and KEGG pathway identifiers were generated using an InterProScan (v. 5.2.45)[60] analysis and available in ORCAE. More specifically, gene functional descriptions were added either manually by consortium expert scientists or automatically through sequence homology searches. The automated method relies on the EC (Enzyme Commission) number reported by InterProScan to retrieve the enzyme name with BLASTP search against UniProtKB/Swiss-Prot[61] to filter out hits that are below 60% identity and 70% query/hit coverage. Although such high stringency on per cent identity and sequence coverage reduced the available number of functional descriptions, it reduced the false-positive prediction rate, as desired here.

Construction of age distributions and WGD analyses. K_S-based age distributions were constructed as previously described[62]. In brief, the K_S values between genes were obtained through maximum likelihood estimation using the CODEML program[63] of the PAML package (v. 4.4c)[64]. Gene families for which K_S estimates between members did not exceed a value of 5 were subdivided into subfamilies. For each duplicated gene in the resulting phylogenetic gene tree, obtained by PhyML[65], all m K_S estimates between the two child clades were added to the K_S distribution with a weight $1/m$ (where m is the number of K_S estimates for a duplication event), so that the weights of all K_S estimates for a single duplication event summed to one. Mixture modelling was used to confirm a WGD signature in the K_S distribution (Fig. 2 and Supplementary Fig. 4.1), for which all duplicates with K_S values ≤0.1 were excluded to avoid the incorporation of allelic and/or splice variants, while all duplicates with K_S values > 2.0 were removed because K_S saturation and stochasticity can mislead mixture modelling above this range[62]. For further details see Supplementary Note 4.1.

Absolute dating of the identified WGD event was performed as described previously[13,29]. In brief, paralogueous gene pairs located in duplicated segments (anchors) and duplicated pairs lying under the WGD peak (peak-based duplicates) were collected for phylogenetic dating. Anchors, assumed to be corresponding to the most recent WGD, were detected using i-ADHoRe 3.0 (refs 66,67). Only a low number of duplicated segments and hence anchors could be identified, most likely because of the fragmented assembly of *Z. marina.* However, the identified anchors did confirm the presence of a broad WGD peak between a K_S of 0.8 and 1.6 (data not shown). For each WGD paralogueous pair, an orthogroup was created that included the two paralogues plus several orthologues from other plant species as identified by InParanoid (v. 4.1)[68] using a broad taxonomic sampling: one representative orthologue from the order Cucurbitales, two from the Rosales, two from the Fabales, two from the Malpighiales, two from the Brassicales, one from the Malvales, one from the Solanales, two from the Poales, one orthologue from *Musa acuminata*[69] (Zingiberales), and one orthologue from *Spirodela polyrhiza*[11] (Alismatales). In total, about 180 orthogroups from anchor pair duplicates and peak-based duplicates were collected. The node joining the two *Z. marina* WGD paralogues was then dated using the BEAST v. 1.7 package[70] under an uncorrelated relaxed clock model and a LG+G (four rate categories) evolutionary model. A starting tree with branch lengths satisfying all fossil prior constraints was created according to the consensus APGIII phylogeny[71]. Fossil calibrations were implemented using log-normal calibration priors on the following nodes: the node uniting the Malvidae based on the fossil *Dressiantha bicarpellata*[72] with prior offset = 82.8, mean = 3.8528, and s.d. = 0.5)(ref. 73), the node uniting the Fabidae based on the fossil *Paleoclusia chevalieri*[74] with prior offset = 82.8, mean = 3.9314, and s.d. = 0.5(ref. 75), the node uniting the Alismatales (including *Z. marina* and *Spirodela polyrhiza*) with the other monocots based on the oldest fossil monocot pollen, *Liliacidites*[76,77] from the Trent's Reach locality, with prior offset = 125, mean = 2.0418, and s.d. = 0.5 (refs 14,78) and the root with prior offset = 124, mean = 4.0786, and s.d. = 0.5 (ref. 79). The offsets of these calibrations represent hard minimum boundaries, while their means represent locations for their respective peak mass probabilities in accordance with some of the most recent and taxonomically complete dating studies available for these specific clades[14,80]. A run without data was performed to ensure proper placement of the marginal calibration prior distributions[81]. The Markov chain Monte Carlo (MCMC) for each orthogroup was run for 10^6 generations, sampling every 1,000 generations resulting in a sample size of 10^4. The resulting trace files of all orthogroups were evaluated manually using Tracer v. 1.5[70] with a burn-in of 1,000 samples to ensure proper convergence (minimum ESS for all statistics at least 200). In total, 169 orthogroups were accepted and all age estimates for the node uniting the WGD paralogous pairs were then grouped into one absolute age distribution (Fig. 2, too few anchors were available to evaluate them separately from the peak-based duplicates), for which kernel density estimation (KDE) and a bootstrapping procedure were used to find the peak consensus WGD age estimate and its 90% confidence interval boundaries, respectively.

Intra- and inter-genomic co-linearity was investigated (Supplementary Tables 4.2 and 4.3) using MCScanX[82] based on a BLASTP search of all genomic protein coding genes with an E-value cut-off of e^{-10}. Only one large duplicated segment was detected, which was most likely due to the fragmented assembly of *Z. marina*; only 27 scaffolds had a size larger than 1 Mb, accounting for only 23.4% of all protein-coding genes. We therefore additionally used i-ADHoRe (v. 3.0)[66] to investigate genomic co-linearity by including all possible scaffolds.

Gene family comparisons. Protein sets were collected for 14 species: *Z. marina* (ORCAE v. 2.1), *Arabidopsis thaliana* (TAIR10), *Thellungiella parvula* (http://thellungiella.org) *Populus trichocarpa* (Phytozome v. 9.0), *Vitis vinifera* (Phytozome v. 9.0), *Amborella trichopoda* (http://amborella.huck.psu.edu), *Oryza sativa* japonica (Phytozome v. 9.0), *Zea mays* (Phytozome v. 9.0), *Brachypodium distachyon* (Phytozome v. 9.0), *Spirodela polyrhiza* (http://mocklerlab.org), *Selaginella moellendorffii* (Phytozome v. 9.0), *Physcomitrella patens* (Phytozome v. 9.0), *Chlamydomonas reinhardtii* (Phytozome v. 9.0), and *Ostreococcus lucimarinus* (ORCAE v. 6/3/2013). These species were selected in order to provide a phylogenetic representation traversing green algae, basal plants, monocots, and dicots. Following an 'all-vresus-all' TimeLogic Decypher Tera-BLASTP (Active Motif Inc.; e-value threshold $1 \times e^{-3}$, max hits 500) comparison, OrthoMCL (v. 2.0; mcl inflation factor 3.0)[83] was used to delineate gene families. Confidence in establishing gene losses in *Zostera* was enhanced by using a combination of reciprocal blast, TblastN, re-annotation of *Spirodela* (and other monocot genes), and careful phylogenetic analysis. OrthoMCL results and related protein resources are available in the ORCAE download section.

To further understand gene family expansion or contraction in *Z. marina* in comparison with other sequenced genomes, gene family sizes were calculated for all gene families (excluding orphans and species-specific families) (Supplementary Note 4.2). The number of genes per species for each family was transformed into a matrix of z-scores in order to centre and normalize the data. The first 100 families with the largest gene family size in *Z. marina* were selected. The z-score profile was hierarchically clustered (complete linkage clustering) using Pearson correlation as a distance measure. The functional annotation of each family was predicted based on sequence similarity to entries in the InterProScan and Pfam protein domain database where more than 30% of proteins in the family share the same protein domain. The phylogenetic profile and phylogenetic tree topology provided at PLAZA[84] were used to reconstruct the most parsimonious series of gene gain and loss events. The Dollop program from the PHYLIP package[85] was used to determine the minimum gene set at ancestral nodes of the phylogenetic tree. The Dollop program is based on the Dollo parsimony principle, which assumes that novel gene families arise exactly once during evolution but can be lost independently in different phylogenetic lineages.

Search for presence/absence of orthologues for specific genes and families. A dedicated search for orthologues/homologues was performed for genes and proteins involved in stomata differentiation (Supplementary Note 5.1), volatile biosynthesis and sensing with focus on ethylene and terpenes (Supplementary Note 6.1), as well as genes involved in male flower specification and pollen

differentiation (Supplementary Note 11.1). To this end, queries were chosen from documented genes involved in these pathways (usually from *Arabidopsis* but occasionally from *Oryza*, *Zea* and tomato). Next, the search for homologues in *Zostera marina*, *Spirodela polyrhiza*, *Oryza sativa japonica* and *Arabidopsis thaliana* (when not used as a query) was performed using BLASTP. To avoid missing or poorly annotated genes a TBLASTN search was conducted using the above queries against the *Zostera marina* and *Spirodela polyrhiza* genomes. Putative orthologues were identified based on reciprocal BLASTP searches with *Arabidopsis* (or the other queries). Owing to species-specific duplications, this may produce some paralogous genes to appear orthologous to the query, or vice versa (see Extended Data Tables 1–3). To further confirm correct orthology assignments, phylogenetic trees were built using a broader sampling of protein sequences from both the query species and the three target species. Ambiguously aligned sequences (especially due to indels) were checked manually and corrected or removed.

30. Olsen, J. L. *et al.* Eelgrass *Zostera marina* populations in northern Norwegian fjords are genetically isolated and diverse. *Mar. Ecol. Prog. Ser.* **486,** 121–132 (2013).
31. den Hartog, C., Hennen, J., Noten, T. M. P. A. & Van Wijk, R. J. Chromosome numbers of the European seagrasses. *Plant Syst. Evol.* **156,** 55–59 (1987).
32. Kuo, J. Chromosome numbers of the Australian Zosteraceae. *Plant Syst. Evol.* **226,** 155–163 (2001).
33. Reusch, T. B. H. & Bostrom, C. Widespread genetic mosaicism in the marine angiosperm *Zostera marina* is correlated with clonal reproduction. *Evol. Ecol.* **25,** 899–913 (2010).
34. Doyle, J. J. & Doyle, J. L. Isolation of plant DNA from fresh tissue. *Focus* **12,** 13–15 (1990).
35. Jaffe, D. B. *et al.* Whole-genome sequence assembly for mammalian genomes: Arachne 2. *Genome Res.* **13,** 91–96 (2003).
36. Smit, A. & Hubley, R. in *RepeatModeler Open-1.0* (Repeat Masker Website, http://www.repeatmasker.org/ 2010).
37. Maumus, F. & Quesneville, H. Deep investigation of *Arabidopsis thaliana* junk DNA reveals a continuum between repetitive elements and genomic dark matter. *PLoS ONE* **9,** e94101 (2014).
38. Flutre, T., Duprat, E., Feuillet, C. & Quesneville, H. Considering transposable element diversification in *de novo* annotation approaches. *PLoS ONE* **6,** e16526 (2011).
39. Quesneville, H. *et al.* Combined evidence annotation of transposable elements in genome sequences. *PLOS Comput. Biol.* **1,** e22 (2005).
40. Hoede, C. *et al.* PASTEC: an automatic transposable element classification tool. *PLoS ONE* **9,** e91929 (2014).
41. Grabherr, M. G. *et al.* Full-length transcriptome assembly from RNA-Seq data without a reference genome. *Nature Biotechnol.* **29,** 644–652 (2011).
42. Gouzy, J., Carrere, S. & Schiex, T. FrameDP: sensitive peptide detection on noisy matured sequences. *Bioinformatics* **25,** 670–671 (2009).
43. Li, B. & Dewey, C. N. RSEM: accurate transcript quantification from RNA-Seq data with or without a reference genome. *BMC Bioinformatics* **12,** 323 (2011).
44. Li, W. & Godzik, A. Cd-hit: a fast program for clustering and comparing large sets of protein or nucleotide sequences. *Bioinformatics* **22,** 1658–1659 (2006).
45. Trapnell, C., Pachter, L. & Salzberg, S. L. TopHat: discovering splice junctions with RNA-Seq. *Bioinformatics* **25,** 1105–1111 (2009).
46. Falcon, S. & Gentleman, R. Using GOstats to test gene lists for GO term association. *Bioinformatics* **23,** 257–258 (2007).
47. Zhang, L. *et al.* A genome-wide characterization of microRNA genes in maize. *PLoS Genet.* **5,** e1000716 (2009).
48. Jiang, H. & Wong, W. H. SeqMap: mapping massive amount of oligonucleotides to the genome. *Bioinformatics* **24,** 2395–2396 (2008).
49. Meyers, B. C. *et al.* Criteria for annotation of plant microRNAs. *Plant Cell* **20,** 3186–3190 (2008).
50. Addo-Quaye, C., Miller, W. & Axtell, M. J. CleaveLand: a pipeline for using degradome data to find cleaved small RNA targets. *Bioinformatics* **25,** 130–131 (2009).
51. Degroeve, S., Saeys, Y., De Baets, B., Rouze, P. & Van de Peer, Y. SpliceMachine: predicting splice sites from high-dimensional local context representations. *Bioinformatics* **21,** 1332–1338 (2005).
52. Foissac, S. *et al.* Genome annotation in plants and fungi: EuGene as a model platform. *Curr. Bioinformatics* **3,** 87–97 (2008).
53. Van Bel, M. *et al.* Dissecting plant genomes with the PLAZA comparative genomics platform. *Plant Physiol.* **158,** 590–600 (2012).
54. Abeel, T., Van Parys, T., Saeys, Y., Galagan, J. & Van, P. GenomeView: a next-generation genome browser. *Nucleic Acids Res.* **40,** e12 (2012).
55. Ter-Hovhannisyan, V., Lomsadze, A., Chernoff, Y. O. & Borodovsky, M. Gene prediction in novel fungal genomes using an ab initio algorithm with unsupervised training. *Genome Res.* **18,** 1979–1990 (2008).
56. Stanke, M., Tzvetkova, A. & Morgenstern, B. AUGUSTUS at EGASP: using EST, protein and genomic alignments for improved gene prediction in the human genome. *Genome Biol.* **7,** S11 (2006).
57. Lowe, T. M. & Eddy, S. R. tRNAscan-SE: A program for improved detection of transfer RNA genes in genomic sequence. *Nucleic Acids Res.* **25,** 955–964 (1997).
58. Burge, S. W. *et al.* Rfam 11.0: 10 years of RNA families. *Nucleic Acids Res.* **41,** D226–D232 (2013).
59. Sterck, L., Billiau, K., Abeel, T., Rouzé, P. & Van der Peer, Y. ORCAE: online resource for community annotation of eukaryotes. *Nature Methods* **9,** 1041 (2012).
60. Mitchell, A. *et al.* The InterPro protein families database: the classification resource after 15 years. *Nucleic Acids Res.* **43,** D213–D221 (2015).
61. The UniProt Consortium. UniProt: a hub for protein information. *Nucleic Acids Res.* **43,** D204–D212 (2015).
62. Vanneste, K., Van de Peer, Y. & Maere, S. Inference of genome duplications from age distributions revisited. *Mol. Biol. Evol.* **30,** 177–190 (2013).
63. Goldman, N. & Yang, Z. A codon-based model of nucleotide substitution for protein-coding DNA sequences. *Mol. Biol. Evol.* **11,** 725–736 (1994).
64. Yang, Z. PAML 4: Phylogenetic analysis by maximum likelihood. *Mol. Biol. Evol.* **24,** 1586–1591 (2007).
65. Guindon, S. *et al.* New algorithms and methods to estimate maximum-likelihood phylogenies: assessing the performance of PhyML 3.0. *Syst. Biol.* **59,** 307–321 (2010).
66. Proost, S. *et al.* i-ADHoRe 3.0-fast and sensitive detection of genomic homology in extremely large data sets. *Nucleic Acids Res.* **40,** e11 (2012).
67. Fostier, J. *et al.* A greedy, graph-based algorithm for the alignment of multiple homologous gene lists. *Bioinformatics* **27,** 749–756 (2011).
68. Ostlund, G. *et al.* InParanoid 7: new algorithms and tools for eukaryotic orthology analysis. *Nucleic Acids Res.* **38,** D196–D203 (2010).
69. D'Hont, A. *et al.* The banana (*Musa acuminata*) genome and the evolution of monocotyledonous plants. *Nature* **488,** 213–217 (2012).
70. Drummond, A. J., Suchard, M. A., Xie, D. & Rambaut, A. 3408070; Bayesian phylogenetics with BEAUti and the BEAST 1.7. *Mol. Biol. Evol.* **29,** 1969–1973 (2012).
71. The Angiosperm Phylogeny Group. An update of the Angiosperm Phylogeny Group classification for the orders and families of flowering plants: APG III. *Bot. J. Linn. Soc.* **161,** 105–121 (2009).
72. Gandolfo, M., Nixon, K. & Crepet, W. A new fossil flower from the Turonian of New Jersey: *Dressiantha bicarpellata* gen. et sp. nov. (Capparales). *Am. J. Bot.* **85,** 964–974 (1998).
73. Beilstein, M. A., Nagalingum, N. S., Clements, M. D., Manchester, S. R. & Mathews, S. Dated molecular phylogenies indicate a Miocene origin for *Arabidopsis thaliana*. *Proc. Natl Acad. Sci. USA* **107,** 18724–18728 (2010).
74. Crepet, W. & Nixon, K. C. Fossil Clusiaceae from the late Cretaceous (Turonian) of New Jersey and implications regarding the history of been pollination. *Am. J. Bot.* **85,** 1122–1133 (1998).
75. Xi, Z. *et al.* Phylogenomics and a posteriori data partitioning resolve the Cretaceous angiosperm radiation Malpighiales. *Proc. Natl Acad. Sci. USA* **109,** 17519–17524 (2012).
76. Doyle, J. A., Endress, P. K. & Upchurch, G. R. Early Cretaceous monocots: a phylogenetic evaluation. *Acta Musei Nationalis Pragae, Series B. Historia Naturalis* **64,** 59–87 (2008).
77. Iles, W. J. D., Smith, S. Y., Gandolfo, M. A. & Graham, S. W. Monocot fossils suitable for molecular dating analyses. *Bot. J. Linn. Soc.* **178,** 346–374 (2015).
78. Janssen, T. & Bremer, K. The age of major monocot groups inferred from 800+ rbcL sequences. *Bot. J. Linn. Soc.* **146,** 385–398 (2004).
79. Smith, S. A., Beaulieu, J. M. & Donoghue, M. J. An uncorrelated relaxed-clock analysis suggests an earlier origin for flowering plants. *Proc. Natl Acad. Sci. USA* **107,** 5897–5902 (2010).
80. Clarke, J. T., Warnock, R. C. & Donoghue, P. C. Establishing a time-scale for plant evolution. *New Phytol.* **192,** 266–301 (2011).
81. Heled, J. & Drummond, A. J. Calibrated tree priors for relaxed phylogenetics and divergence time estimation. *Syst. Biol.* **61,** 138–149 (2012).
82. Wang, Y. *et al.* MCScanX: a toolkit for detection and evolutionary analysis of gene synteny and collinearity. *Nucleic Acids Res.* **40,** e49 (2012).
83. Li, L., Stoeckert, C. J. & Roos, D. S. OrthoMCL: identification of ortholog groups for eukaryotic genomes. *Genome Res.* **13,** 2178–2189 (2003).
84. Proost, S. *et al.* PLAZA 3.0: an access point for plant comparative genomics. *Nucleic Acids Res.* **43,** D974–D981 (2015).
85. Felsenstein, J. in *PHYLIP: Phylogenetic inference program, version 3.6* (University of Washington, 2005).
86. Pillitteri, L. J. & Dong, J. Stomatal development in *Arabidopsis*. *Arabidopsis Book* **11,** e0162 (2013).
87. Lallemand, B., Erhardt, M., Heitz, T. & Legrand, M. Sporopollenin biosynthetic enzymes interact and constitute a metabolon localized to the endoplasmic reticulum of tapetum cells. *Plant Physiol.* **162,** 616–625 (2013).

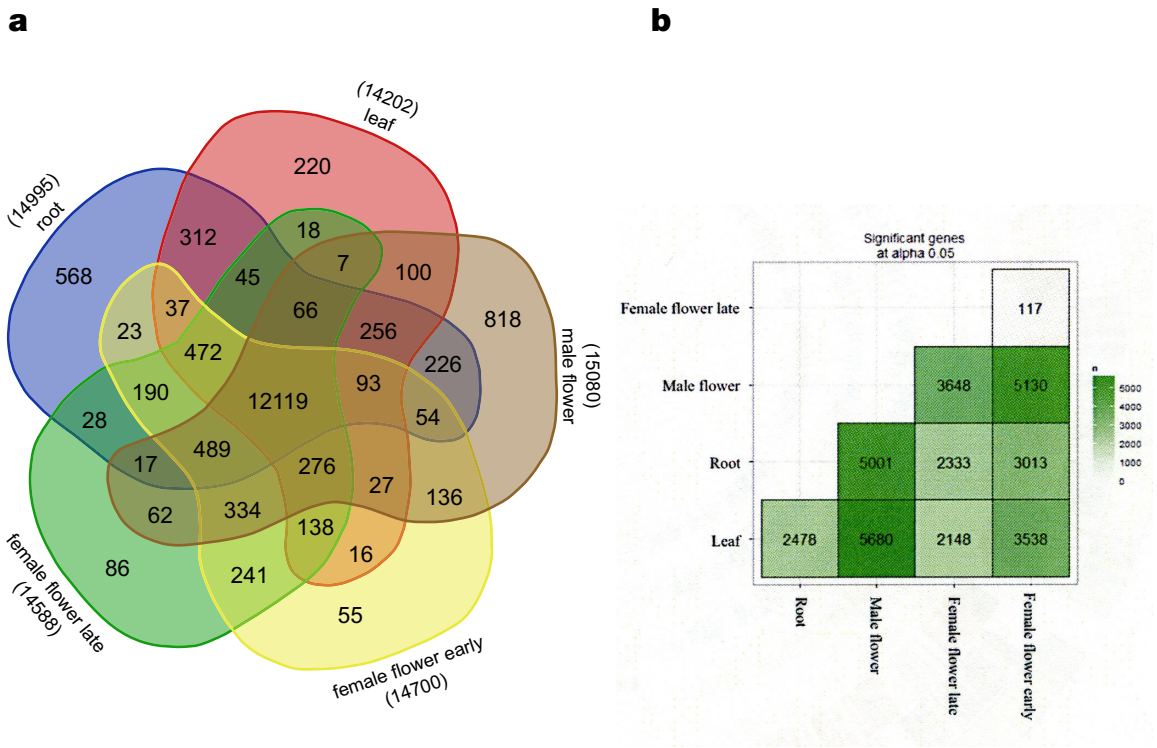

Extended Data Figure 1 | Number of genes expressed in five tissues of *Z. marina*. **a**, Venn diagram of genes with expression values (FPKM) higher than 1 are considered as expressed in the tissue. **b**, Pairwise differential gene expression analysis between tissues. The male flower shows the highest number of differentially expressed genes.

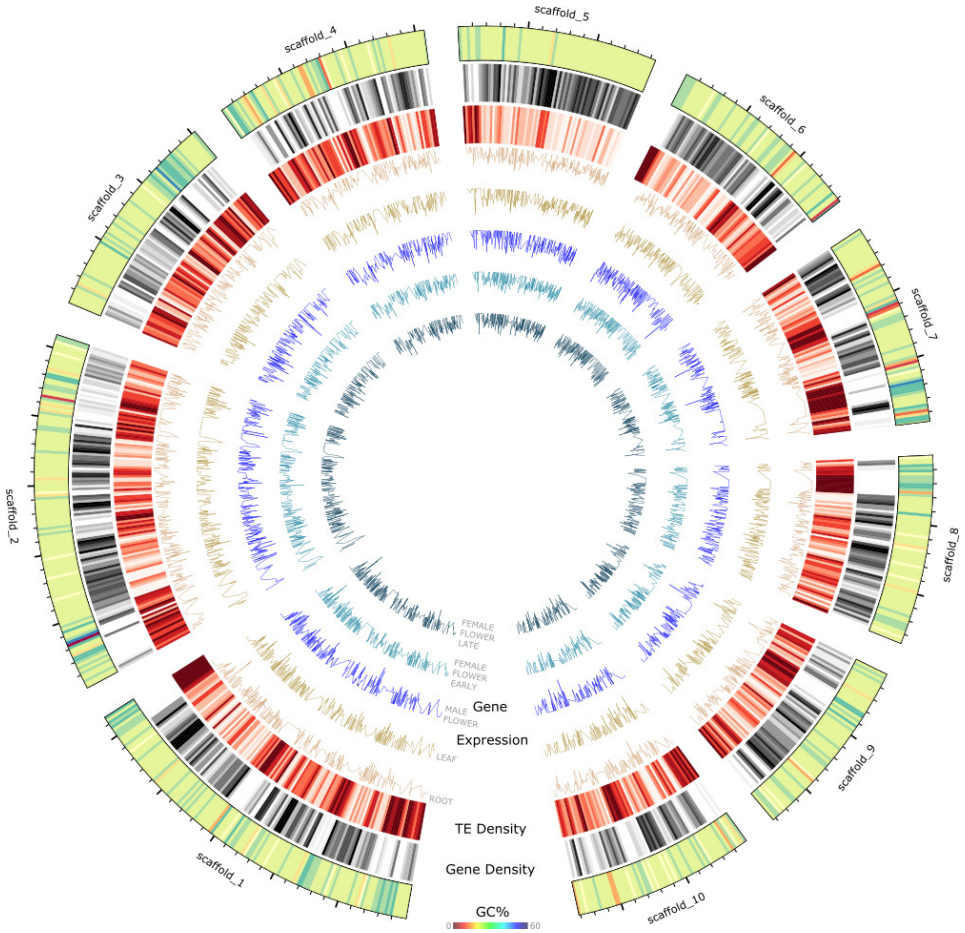

Extended Data Figure 2 | Circos plot of the ten largest scaffolds of *Z. marina*. Tracks from outside to inside. GC percentage, gene density, and transposable element (TE) density (density measured in 20-Kb sliding windows and gene expression profiles from five tissues (root, leaf, male flower, female flower early and female flower late) presented as $\log_2$ FPKM values.

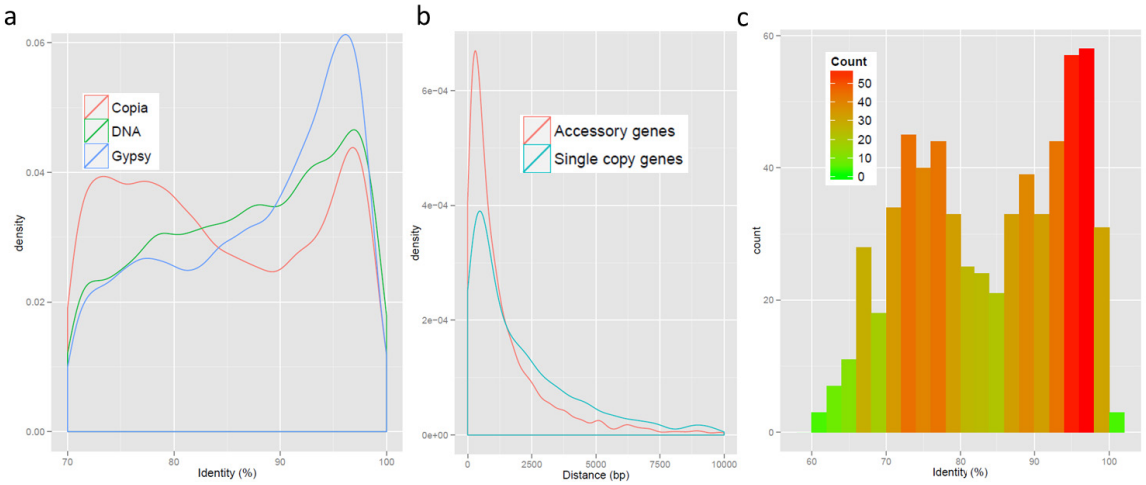

Extended Data Figure 3 | Potential impact of transposable elements (TEs) on *Z. marina* evolution. a, Frequency distribution of pairwise sequence identity values between copies of Copia- and Gypsy-type LTR retrotransposons and DNA transposons, and their cognate consensus sequences (younger repeats share higher sequence similarity). Two peaks are detectable for Copia-type elements. **b**, Distance to the closest TE for the set of *Z. marina* single-copy genes and the set of *Z. marina* accessory genes. TE-proximal accessory genes are more frequent than TE-proximal single-copy genes. **c**, Frequency of pairwise sequence identity between accessory gene-proximal Ty3-Gypsy elements and their cognate consensus sequences. A number of high-identity copies (that is, putatively young duplicate genes) is observed.

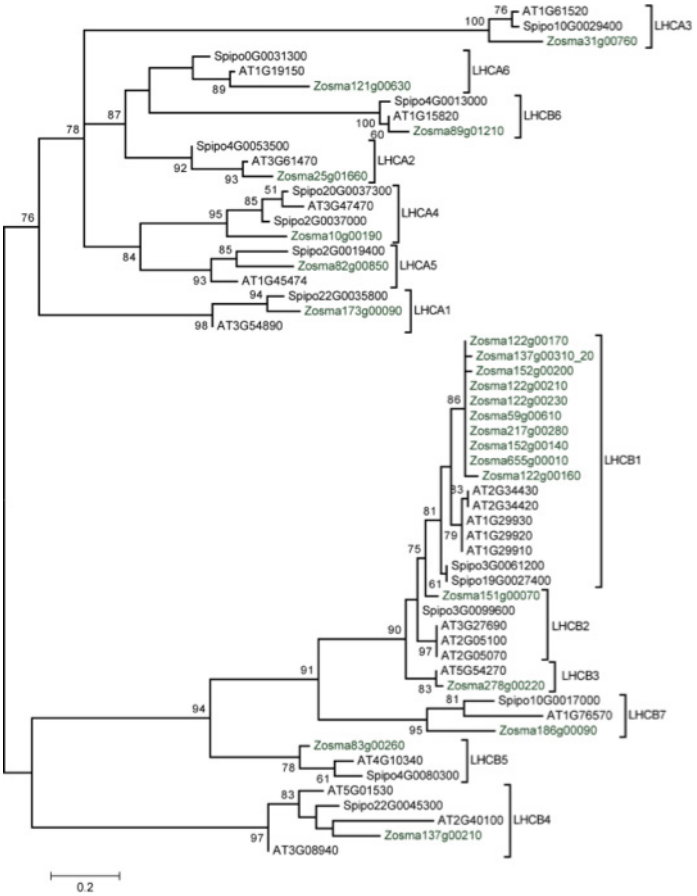

Extended Data Figure 4 | Unrooted maximum likelihood tree of genes encoding light-harvesting complex A (LHCA) and LHCB proteins of *Z.marina*, *Spirodela polyrhiza* and *Arabidopsis thaliana*. The analysis was carried out on protein sequences using PhyML 3 with LG substitution model and 100 bootstrap replicates. Supplementary Note 7.1, Supplementary Table 7.3.

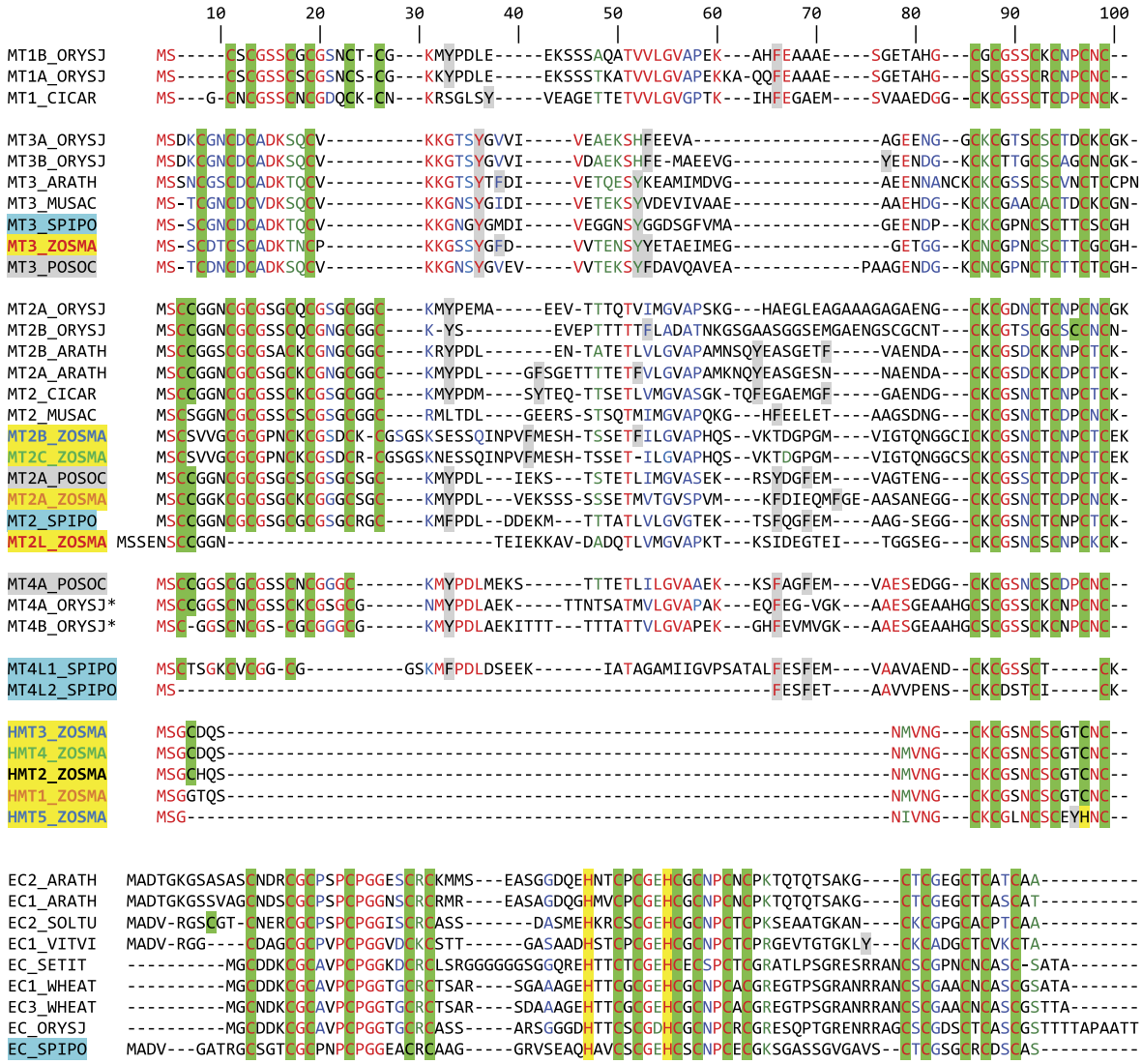

Extended Data Figure 5 | Alignment of metallothionein (MT) and half-metallothionein (HMT) genes in *Z. marina* as compared with other plants. Alignments were performed in ClustalW on the Lyon PBIL web server and edited manually. The upper alignments are for type 1–3 MTs and HMTs; the lower alignment is for type 4 EcMTs where there is no *Zostera* homologue. Conserved residues are shown in red and residues in the same amino acid group in blue. Cys and His residues, putatively involved in binding metals, are highlighted in green and yellow, respectively. Aromatic amino acids absent in canonical animal MTs are highlighted in grey. MTs and MT-like proteins were obtained from: *Arabidopsis thaliana* (ARATH), Japanese rice (ORYSJ), *Cicer arietinum* (CICAR), banana (MUSAC), wheat (WHEAT), potato (SOLTU), *Setaria Italica* (SETIT), *Vitis vinifera* (VITVI) and the alismatids: *Posidonia oceanica* (POSOC) highlighted in grey, *Spirodela polyrhiza* (SPIPO) highlighted in blue, and *Zostera marina* (ZOSMA) highlighted in yellow. See Supplementary Note 8.2.

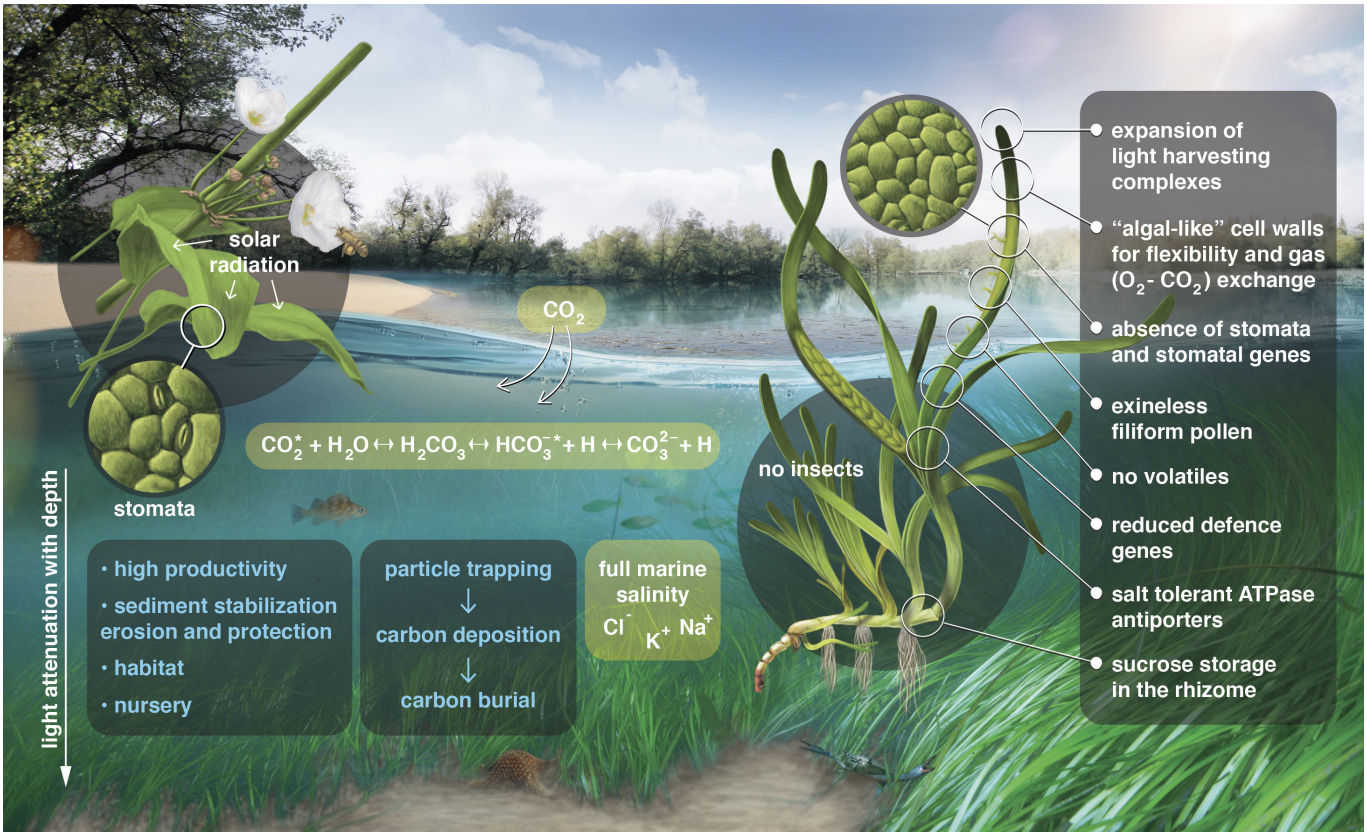

Extended Data Figure 6 | Conceptual summary of physiological and structural adaptations made by *Z. marina* in its return to the sea. Ecosystem services shown in blue. Physical processes related to salinity, light and CO_2 availability shown in white within light-green boxes. Gene losses and gains associated with morphological and physiological processes shown in white within the dark-green box on the right.

Extended Data Table 1 | Genes involved in stomata development in *Z. marina* compared to other angiosperms

Gene Name	Symbol	*A. thaliana*	O. sativa	*S. polyrhiza*	*Z. marina*
Differentiation Genes					
SPEECHLESS	SPCH	At5g53210	Os02g15760 Os06g33450	Sp6G0039300	NF-1
MUTE	MUTE	At3g06120	Os05g51820		NF-1
FAMA	FAMA	At3g24140	Os05g50900		NF-1
SCREAM / ICE1	SCRM	At3g26744	Os11g32100	Sp4G0062100	Zm11g00170
SCREAM2 / ICE2	SCRM2	At1g12860	Os01g70310	Sp0G0129300	NF-1
FOUR LIPS MYB88	FLP MYB88	At1g14350 At2g02820	Os07g43420	Sp0G0157900	NF-1
Spacing & Patterning Genes					
ERECTA	ER	At2g26330	Os06g10230	Sp15G0047400	Zm87g00130 Zm292g00090
ERECTA-LIKE1 ERECTA-LIKE2	ERL1 ERL2	At5g62230 At5g07180	Os06g03970	Sp11G0029800	Zm85g01030
TOO MANY MOUTHS	TMM	At1g80080	Os01g43440	Sp18G0010300	NF-2
STOMATAL DENSITY & DISTRIBUTION	SDD1	At1g04110	Os03g04950	Sp1G0013100	NF-1
CO2 RESPONSE SECRETED PROTEASE	CRSP	At1g20160	Os09g30458	Sp3G0019800	Zm58g00010
EPIDERMAL PATTERNING FACTOR1	EPF1	At2g20875	Os04g54490	Sp14G0058800	NF-1
EPIDERMAL PATTERNING FACTOR2	EPF2	At1g34245	Os04g38470	Sp15G0006400	NF-1
STOMAGEN/EPF-LIKE9	EPFL9	At4g12970	Os01g68598	Sp7G0057500	NF-1
CHALLAH/EPF-LIKE6	CHAL/EPFL6	At2g30370	Os01g60900 Os05g39880	Sp29G0014100	Zm270g00140
CHAL-LIKE1/EPF-LIKE5	CHALL1/EPFL5	At3g22820	Os03g06610	Sp2G0017500	Zm95g00050
CHAL-LIKE2/EPF-LIKE4	CHALL2/EPFL4	At4g14723	Os11g37190	Sp24G0023900	Zm289g00040
Polarity & Division Asymmetry Genes					
BREAKING OF ASYMMETRY IN THE STOMATAL LINEAGE	BASL	At5g60880	NC*	NC*	NC*
PANGLOSS1	PAN1†	At2g42290 At3g57830	Os08g39590	Sp12G0035200	Zm293g00080
PANGLOSS2	PAN2†	At4g20940	Os07g05190	Sp32G0009300 Sp0G0142000	Zm30g00950 Zm117g00680
POLAR LOCALIZATION DURING ASYMMETRIC DIVISION AND REDISTRIBUTION	POLAR	At4g31805	Os02g55190	Sp10G0014700	Zm16g01600
Cytokinesis Genes					
STOMATAL CYTOKINESIS DEFECTIVE 1	SCD1	At1g49040	Os01g39380	Sp21G0025200	Zm40g00290 Zm40g00310

The genes documented to be involved in stomatal development in *Arabidopsis*[86] were used as queries to find orthologues in rice and *Siprodela polyrhiza* (duckweed). See Supplementary Note 5.1, Supplementary Fig. 5.1 for sequence alignment and phylogenetic tree. NF-1, not found, supported by phylogeny; NF-2, not found, unambiguous reciprocal BlastP; NC, not conserved.
*BASL is not evolutionarily conserved, precluding the finding of its homologue in monocots, if it would exist.
†PAN genes have been searched for using the documented PAN1 and PAN2 genes from maize as baits.

Extended Data Table 2 | Ethylene-responsive transcription factor genes (ERF) in *Zostera marina*

Gene Family	*A. thaliana*	*O. sativa*	*S. polyrhiza*	*Z. marina*	Tissue expression in *Z. marina* (FPKM)				
ACS / ACSL					FFE	FFL	MF	R	L
1-aminocyclopropane-1-carboxylate synthase	AtACS1 AtACS2 AtACS6	OsACS2	NF	NF-1					
	AtACS7	OsACS5 OsACS6 OsACS7	NF	NF-1					
	AtACS4 AtACS5 AtACS8 AtACS9 AtACS11	OsACS1	Sp24g0002100	NF-1					
ACS- like	AtACS10 AtACS12	OsACS12	Sp1g0093100	Zm85g01020	8.7	16.7	16.3	11.3	18.1
AC0					FFE	FFL	MF	R	L
1-aminocyclopropane-1-carboxylate oxidase	AtACO1	Os06g37590 Os01g39860	Sp23g0011700	NF-1					
	AtACO2 AtACO3 AtACO4	Os02g53180 Os09g27750 Os09g27820	NF-1	NF-1					
	AtACO5	Os05g05680 Os11g08380	NF-1	NF-1					
ETR, ERS, EIN4					FFE	FFL	MF	R	L
Ethylene Receptors	AtETR1 AtERS1	Os03g49500 Os05g06320	Sp6G0049300 Sp22g0015200	NF-1					
	AtEIN4 AtETR2 AtERS2	Os04g08740 Os02g57530 Os07g15540	Sp1g0021500 Sp23g0013000	NF-1					
CTR1, EIN2 & Co					FFE	FFL	MF	R	L
Signaling genes and interacting partners	AtCTR1	Os02g32610 Os09g39320	Sp0g0009700	NF-1					
	AtEDR1	Os03g06410	NF-1	Zm289g00100	17.7	13.1	11.9	22.4	22.5
	AtEIN2	Os07g06130* Os03g49400*	Sp8g0029200	NF-1					
	AtRTE1	Os01g51430 Os05g46240	Sp14g0010800	NF-1					
	AtRTH	Os03g58520	Sp2g0051000	Zm159g00460	16.4	23.5	29.9	31.2	33
	AtRAN1	Os02g07630 Os06g45500	Sp8g0019500	Zm56g01580	10.8	16.7	15.2	72	35
	AtHMA5	Os04g46940 Os02g10290	Sp12g0033200	Zm25g00180	3.1	6	26.4	19.3	2.8
	AtEIN3	Os07g48630 Os03g20780	Sp3g0015900	Zm44g00270	11	19.8	115	124	70
	AtEIL1	Os03g20790	Sp0g0106000	Zm140g00280	2	0.4	0.8	0	2.7
	AtEBF1 AtEBF2	Os02g10700 Os06g40360	Sp21g0000800 Sp27g0021100 Sp27g0021200	NF-1					
	AtXRN4	Os03g58060	Sp2g0012600	Zm177g00170	15.6	10.3	13.4	16.9	20.2

MF, male flowers; FFE, female flowers early; FFL, female flowers late; R, roots; L, leaves; NF-1, not found as supported by reciprocal Blast and phylogeny. See Supplementary Note 6.1, Supplementary Fig. 6.1 for sequence alignment and phylogenetic tree. Grey indicates genes not involved in ethylene biosynthesis and signal pathways but strongly co-expressed, indicative of multiple functions.

Extended Data Table 3 | Genes involved in pollen development of *Z. marina* compared to other angiosperms

Gene Name	Symbol	*A. thaliana*	*O. sativa*	*S. polyrhiza*	*Z. marina*	Tissue expression in *Z. marina* (FPKM)				
						FFE	FFL	MF	R	L
ACYL-COA SYNTHETASE 5	ACOS5	At1g62940	Os04g24530	Sp12g0064500	NF-1					
POLYKETIDE SYNTHASE A	PKSA (LAP6)	At1g02050	Os10g34360	Sp16g0013800	NF-1					
POLYKETIDE SYNTHASE B	PKSB (LAP5)	At4g34850	Os07g22850	Sp1g0062300	NF-1					
LESS ADHERENT POLLEN 3	LAP3	At3g59530	Os03g15710	Sp16g0030000	NF-1					
TETRAKETIDE a-PYRONE REDUCTASE 1	TKPR1 (DRL1)	At4g35420	Os08g40440	Sp10g0016700	NF-1					
TETRAKETIDE a-PYRONE REDUCTASE 2	TKPR2 (CCRL6)	At1g68540	Os01g03670	NF	NF-1					
CYTOCHROME P450 704B1/2	CYP704B 1(CYP704 B23)	At1g69500	Os03g07250	Sp2g0036600	Zm149g00275	NA	NA	NA	NA	NA
TYPE III LIPID TRANSFER PROTEINS	LTP3	At5g62080 At5g07230 At5g52160	Os08g43290 Os09g35700	Sp16g0007800	NF-1					
GA-regulated Myb-like Transcription Factor	GAMYB (MYB65 MYB33)	At3g11440 At5g06100	Os01g59660	Sp22g0020200	Zm6g00090	8.8	6.6	26.9	3.1	4.3
FACELESS POLLEN-1, ECERIFERUM 3	FLP1 (ERC3, WAX2)	At5g57800	Os09g25850 Os02g08230 Os06g44300	Sp5g0009000	NF-1					
INAPERTURATE POLLEN 1	INP1	At4g22600	Os02g44250	Sp13g0036900	NF-2					
GLYCOSYLTRANSFERASE 1	GT1	At1g19710 At1g75420	Os01g15780	Sp14G0031700	Zm69g00440	10.1	8.1	41.7	224.1	62.4
CYSTEINE ENDOPEPTIDASE 1	CEP1	At5g50260	Os08g44270 Os11g14900	Sp4g0036900 Sp11g0013300	NF-1					
MALE STERILE 188	MS188 (MYB80)	At5g56110	Os04g39470	Sp4g0087200	Zm262g00100	5.9	4.6	42.5	9.4	2.8
Fatty Acyl Thioesterase B	FATB	At1g08510	Os06g05130	Sp21g0008900	Zm1g01370	115.1	104.8	213.7	129.3	124.3
Glycosyl transferase family GT31	B3GALT7	At1g77810	Os02g35870	Sp4g0008000	Zm155g00180	4.4	1.4	354.3	10.5	2.2
NO EXINE FORMATION	NEF1	At5g13390	Os11g32470	Sp9g0054300	Zm5g01490	28.4	23.6	14.7	25.3	18.8

The five genes encoding proteins associated on the ER-located sporopollenin metabolon in *Arabidopsis*[87] are highlighted in grey. The genes documented to be involved in pollen development in *Arabidopsis* or in rice were used as queries to find orthologues. MF, male flowers; FFE, female flowers early; FFL, female flowers late; R, roots; L, leaves; NF-1, not found, supported by reciprocal Blast and phylogeny; NF-2, not found, single copy gene; amb, ambiguous with homologues too similar to point to a specific orthologue. See Supplementary Note 11.1, Supplementary Fig. 11.1 for sequence alignment and phylogenetic tree; Supplementary Table 11.1 for complete gene list.